Nonequilibrium dynamics in an amorphous solid

Sunil P. Singh and Shankar P. Das
School of Physical Sciences, Jawaharlal Nehru University, New Delhi 110067, India

(Received 4 August 2008; revised manuscript received 5 February 2009; published 23 March 2009)

The nonequilibrium dynamics of an amorphous solid is studied with a soft-spin model. We show that the aging behavior in the glassy state follows a modified Kohlrausch-Williams-Watts form similar to that obtained in Lunkenheimer *et al.* [Phys. Rev. Lett. **95**, 055702 (2005)] from analysis of the dielectric loss data. The nature of the fluctuation-dissipation theorem violation is also studied in time as well as correlation windows.

DOI: 10.1103/PhysRevE.79.031504 PACS number(s): 64.70.P−, 05.10.−a, 75.10.Nr, 77.22.Gm

In the glassy state, liquid behaves like a frozen solid with the motion of its constituent particles being localized around randomly distributed sites. Analysis of the dynamics in this nonequilibrium glassy state reveals a variety of phenomena such as aging and memory effects [1,2]. Important progress in understanding the nonequilibrium dynamics of the disordered systems has been made in recent years from study of simple mean-field spin-glass models. In the multispin interaction models, the nonlinearities in the Langevin dynamics give rise [3] to a ergodic-nonergodic (ENE) transition. The basic mechanism for this transition is very similar to that present in the models for the dynamics of supercooled liquids [4]. The seminal work of Ref. [5] dealt with the problem of weak ergodicity breaking [6] in a spherical p-spin ($p>2$) interaction model [7] over the asymptotic time scales. Here the crossing over of the dynamics from a regime of time translational invariance to that of aging behavior was demonstrated analytically [8]. Low-temperature properties of glassy systems, e.g., thermal conductivity and specific heat, have also been studied with models [9] for the structural glass built in terms of a standard Hamiltonian involving spins. In the present paper, we study a soft-spin-type model, which is defined in terms of the displacements of the particles around a corresponding set of random lattice points. We show that the aging behavior in the nonequilibrium glassy state follows a modified Kohlrausch-Williams-Watts (MKWW) form similar to that obtained in Ref. [10] from analysis of the dielectric loss data for several materials below the glass transition temperature T_g.

We consider a model Hamiltonian, which has a translationally invariant form in terms of the displacement variables u_i around an amorphous structure,

$$H = \sum_{p=2}^{\infty} \sum_{i \neq j} J_{ij}^{(p)} (u_i - u_j)^p. \tag{1}$$

For the amorphous solid, the interaction matrix $J_{ij}^{(p)}$ is assumed to be random following a Gaussian probability distribution of zero mean and variance J_p^2/N. The microscopic basis for such a model for an amorphous solid is discussed further below. The time evolution of $u_i(t)$ is given by the dissipative Langevin equation,

$$\Gamma_0^{-1} \frac{\partial u_i}{\partial t} = -\beta \frac{\delta H}{\delta u_i} - z(t) u_i + \xi_i(t), \tag{2}$$

where Γ_0 is the bare kinetic coefficient related to the variance of the Gaussian white noise ξ_i through the fluctuation-dissipation relation $\langle \xi_i(t) \xi_j(t') \rangle = 2\beta^{-1}\Gamma_0 \delta_{ij} \delta(t-t')$. For maintaining the solid state a constraint on the sum of the squares of the u_i's is imposed. In the present context of the amorphous solid state this is equivalent to having a constant Lindemann parameter at a fixed temperature T. In Eq. (2), $z(t)$ is a Lagrange's multiplier used to enforce the constraint $N^{-1}\Sigma_i \langle u_i^2(t) \rangle = 1$. We consider in the present work the nonlinear dynamics keeping in H the contributions from the $p=2$ and 3 terms of expansion (1). This will be referred to as the $p23$ model from hereon.

The time correlation and response functions of the displacement variable u_i are obtained using the standard Martin-Siggia-Rose (MSR) [11] field theory. The field $\hat{u}_i$ conjugate to u_i is introduced in this regard to average over the Gaussian noise ξ_i. The two time-correlation and response functions are, respectively, defined as $C(t,t_w) = N^{-1}\Sigma_{i=1}^{N} \overline{\langle u_i(t) u_i(t_w) \rangle}$ and $R(t,t_w) = N^{-1}\Sigma_{i=1}^{N} \overline{\langle \hat{u}_i(t) u_i(t_w) \rangle}$, where the overbars stand for averages over the random bonds $\{J_{ij}^{(p)}\}$'s and the angular brackets represent mean over the Gaussian white noise ξ_i's. The dynamics of the correlation and response functions are obtained from the equations

$$[\partial_t + z(t)] C(t,t_w) = \int_0^t ds \Sigma(t,s) C(s,t_w) + \int_0^{t_w} ds \Xi'(t,s) R(t_w,s), \tag{3}$$

$$[\partial_t + z(t)] R(t,t_w) = \delta(t-t_w) + \int_{t_w}^t ds \Sigma(t,s) R(s,t_w), \tag{4}$$

where we denote $\Xi'(t,t') = 2\delta(t-t') + \Xi(t,t')$. The kernels are obtained from a perturbative summation as $\Xi(t,t') = \Sigma_P a_p C^{p-1}(t,t')$ and $\Sigma(t,t') = \Sigma_P (p-1) a_p C^{p-2}(t,t') R(t,t')$ in terms of a set of coupling constants $\{a_p\}$, which depend on nonlinearities in the dynamic equations. For the $p23$ model considered here, we obtain up to one loop order $a_2 = 2(\beta J_2)^2$ and $a_3 = 18(\beta J_3)^2$. The necessary boundary conditions for C and R are, respectively, chosen as [5] $R(t,t^-) = 1$ and $\partial_t C(t,t^{\pm}) = \pm 1$. The Lagrange's multiplier $z(t)$, which ensures $C(t,t) = 1$, is obtained as $z(t) = 1 + \int_0^t ds \{\Xi(t,s) R(s,t) + \Sigma(t,s) C(t,s)\}$.

The analysis of the asymptotic dynamics of $C(t,t_w)$ for both t and $t_w \to \infty$ is divided [5] into two main regimes. First, for $(t-t_w)/t \to 0$ the time translational invariance (TTI)

holds. At this stage C and R are related through the fluctuation dissipation theorem (FDT) $R_1(t)=-\Theta(t)\partial_t C_1(t)$, where we denote $C(t+t_w,t_w)\equiv C_1(t)$ and $R(t+t_w,t_w)\equiv R_1(t)$. Second, for $(t-t_w)/t\sim 1$, i.e., for widely separated t and t_w, there is aging behavior. The correlation and response functions, respectively, denoted by C_A and R_A in this case, are assumed to be functions of $t_w/t\equiv\lambda(0<\lambda<1)$. We define $C_A(t,t_w)=q\mathcal{C}(\lambda)$ and $R_A(t,t_w)=t^{-1}\mathcal{R}(\lambda)$. In the limit, $\lambda\to 1$, $\mathcal{C}(\lambda)\to 1$, and $\mathcal{R}(\lambda)\neq 0$. The solutions in the FDT and the aging regimes agree if the long-time limit of $C_1(\tau)$ is q. The latter is termed as the nonergodicity parameter (NEP). In the FDT regime, both Eqs. (3) and (4) reduce to a single equation,

$$(\partial_t+1)C_1(t)+\int_0^t ds\Xi_1(t-s)\partial_s C_1(s)=z_\infty[C_1(t)-1]. \quad (5)$$

The kernel $\Xi_1[C_1]=a_2C_1+a_3C_1^2$ in case of the $p23$ model. Except for the linear term on the right-hand side, Eq. (5) is same as the basic dynamical equation in the self-consistent mode-coupling theory of the structural glass. The latter represents the asymptotic dynamics for the time correlation of the equilibrium density fluctuations in a supercooled liquid. However, in the present case the nontrivial renormalization contribution to the transport coefficient comes from the dissipative nonlinearities in Eq. (2), while in the mode-coupling theory (MCT) for compressible liquids the relevant nonlinearity is in the reversible pressure term. From the $t\to\infty$ limit of Eq. (5) we obtain the following relation:

$$\sum_P a_p(p-1)q^{p-2}+(1-q)^2=0 \quad (6)$$

for the NEP q in terms of the coupling constants a_p.

In the aging regime, the FDT violation is denoted in terms of a parameter x, which is defined through the relation $R_A(t)=x\Theta(t)\partial_t C_A(\tau)$ or equivalently $\mathcal{R}(\lambda)=xq(\partial/\partial\lambda)\mathcal{C}(\lambda)$. We obtain, analyzing Eqs. (3) and (4) in the aging regime, the following relation between x and q:

$$x=-(1-q)\frac{\sum_P a_p(p-2)q^{p-2}}{\sum_P a_p q^{p-1}}. \quad (7)$$

The critical coupling constants $\{a_2^*,a_3^*\}$ for dynamic transition in the $p23$ model are obtained from the solution of Eqs. (6) and (7) as $a_2^*=2/\lambda_0-1/\lambda_0^2$ and $a_3^*=1/\lambda_0^2$, where $\lambda_0=1-q$. The ergodic-nonergodic transition line is given by $a_2^*=2\sqrt{a_3^*}-a_3^*$. This is identical to the line of dynamic transition in the ϕ_{12} model [12] of the mode-coupling theory of structural glass transition. Along the line of transition the parameter λ_0 changes from 0 to 0.5 as the NEP changes from 1 to 0. In the ergodic phase, the NEP $q=0$ and the FDT holds with $x=-1$. Close to the transition line, the relaxation behavior follows several regimes crossing over from power-law decay to a final-stretched exponential form. The corresponding stretching exponent β_α^E is approximated with the empirical relation $\Sigma_p a_p q p^{-1/\beta_\alpha^E}=1$. As ergodicity is restored over the longest time scale, $u(t)$ grows and the spherical constraint is eventually violated. The model with an underlying dynamic transition is thus valid up to the time scales of structural relaxation.

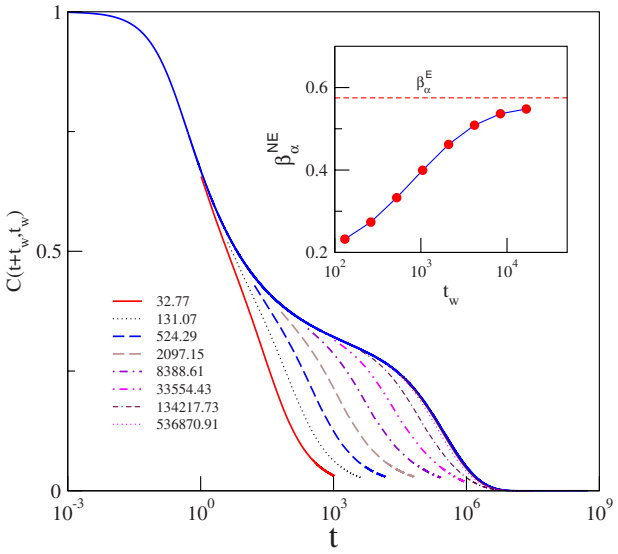

FIG. 1. (Color online) The correlation $C(t+t_w,t_w)$ vs t for a set of waiting times t_w's in the ergodic phase, $a_2=0.82$ and $a_3=2.0$. Inset shows the exponent $\beta_\alpha^{\mathrm{NE}}$ for final stretched exponential relaxation with respect to t_w. Dashed line is the corresponding equilibrium value of stretching exponent.

To get a better understanding of the time scales associated with the aging dynamics in the intermediate time regime and the corresponding FDT violation, we solve Eqs. (3) and (4) numerically. This requires integrating Eqs. (3) and (4) for both t and t_w extending over several time decades. We use the adaptive integration technique [13], which starts with smaller-sized grids for integration over shorter time scales of fast relaxation and correspondingly increases the step size for longer time scales of slow dynamics. In the adaptive integration method of discrete time steps which increases by factor of 4, we are able to cover the range $t_w=2^m\Delta_0$ for $m=15-29$. For $\Delta_0=10^{-3}$, the above range corresponds to $t_w\approx 33-536\,871$. In the ergodic state, at long waiting times t_w the correlation function approaches its equilibrium value, and time translational invariance is eventually reached. In Fig. 1 we display the waiting time dependence of $C(t+t_w,t_w)$ with respect to t for the state $a_2=0.82$ and $a_3=2.02$. In the final stage, the decay follows the stretched exponential form $\exp[-(t/\tau_\alpha^{NE})^{\beta_\alpha^{NE}}]$ with characteristic relaxation time τ_α^{NE} and stretching exponent β_α^{NE}. The inset of Fig. 1 shows β_α^{NE} corresponding to different waiting times t_w. At large t_w, the exponent β_α^{NE} approaches its equilibrium value β_α^E. The latter is determined in terms of a_2 and a_3 using the empirical relation discussed above.

In the nonergodic state, the numerical solution of Eqs. (3) and (4) displays both FDT and aging behavior. In Fig. 2, the time dependence of $C(t+t_w,t_w)$ corresponding to $a_2=0.5$ and $a_3=6.0$ deep in the glassy state is shown for different values of t_w. Initially the correlation decays from 1 to q, and at this stage time translational invariance holds. The dynamics is strongly dependent on t_w at a later stage. The corresponding correlation and response functions for large t_w are scaled

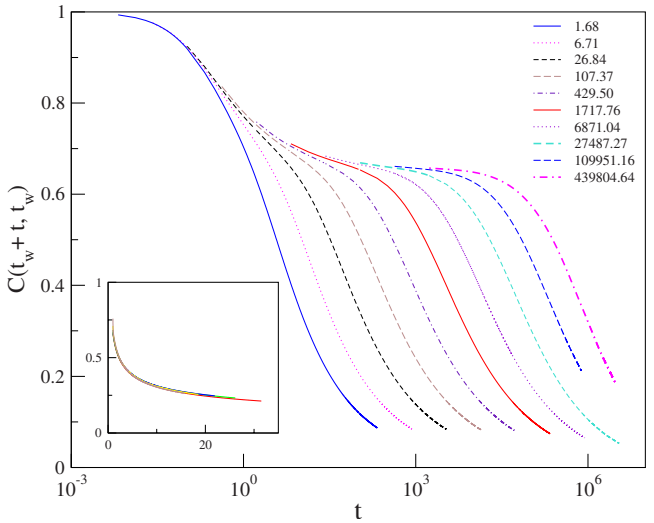

FIG. 2. (Color online) The correlation $C(t+t_w,t_w)$ vs t for a set of waiting times t_w's in the nonergodic phase, $a_2=0.5$ and $a_3=6.0$. Inset shows scaling of different $C(t+t_w,t_w)$'s as a function of $h(t+t_w)/h(t_w)$, where $h(t)\equiv\exp[t^{1-\kappa}/(1-\kappa)]$, with $\kappa=0.96$.

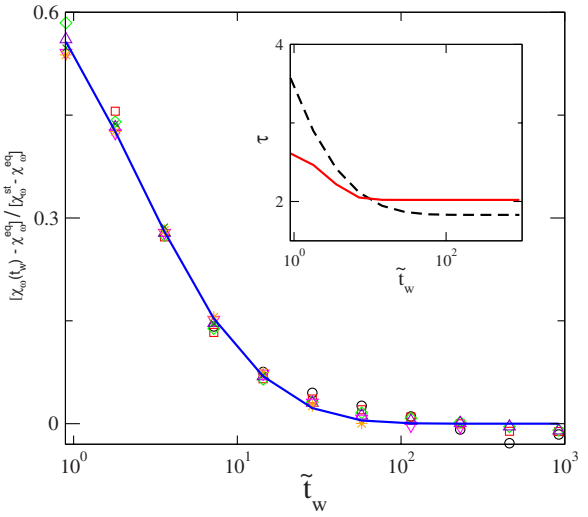

FIG. 3. (Color online) Scaled function $(\chi_\omega(\tilde{t}_w)-\chi_\omega^{\rm eq})/(\chi_\omega^{\rm st}-\chi_\omega^{\rm eq})$ vs $\tilde{t}_w$ for frequencies $\omega=\omega_0 2^{-n}$ with $m=0$ (circle), 2 (square), 4 (diamond), 6 (triangle up), 8 (triangle down), 10 (star), and 12 (cross). $\omega_0=0.13$ in units of Γ_0 (see text). Solid line is a fit to MKWW form (see text) with $\beta=0.50$. Inset show the variation in the $\tau(\tilde{t}_w)$ with $\tilde{t}_w$, following the scheme of Ref. [15] (solid) and Ref. [10] (dashed).

with the ansatz: $C(t+t_w,t_w)=C[h(t+t_w)/h(t_w)]$, where $h(t)$ is a monotonically ascending function of t. The simplest possibility $h(t)=t^\gamma$ is termed as the simple aging and implies $C(t,t_w)\equiv C(t/t_w)$. We adopt here the more general form [14] $h(t)=\exp[t^{1-\kappa}/(1-\kappa)]$. The limit $\kappa\to 0$ implies time translational invariance, while $\kappa\to 1$ represents simple aging, while the case $0<\kappa<1$ is termed as subaging. The dynamics almost conforms to simple aging behavior as shown in the inset of Fig. 2 in which different t_w data overlap on a single master curve having $\kappa=0.96$. This is in agreement with subaging behavior obtained in earlier works [14] on the standard p-spin model. For every t_w, the correlation $C(t+t_w,t_w)$ decays to zero at sufficiently long t. This is termed as weak ergodicity breaking in the aging regime. Since the correlation function in the aging regime approximately depends on the ratio t/t_w (for $\kappa=0.96$), the corresponding Fourier transform $C(\omega,t_w)$ is a function of $\omega t_w\equiv\tilde{t}_w$. We define the response function $\chi_\omega(\tilde{t}_w)\equiv\omega C(\omega,t_w)$. The waiting time $(\tilde{t}_w)$ dependence of $\chi_\omega(\tilde{t}_w)$ for different frequencies *does not* fit with a simple stretched exponential form $\exp[-(t/\tau)^\beta]$ with constant τ over the whole time range and a frequency independent β. On the other hand a good fit is obtained with the MKWW [10] form

$$\chi_\omega(\tilde{t}_w)=[\chi_\omega^{\rm st}-\chi_\omega^{\rm eq}]\exp\{-[\tilde{t}_w/\tau(\tilde{t}_w)]^\beta\}+\chi_\omega^{\rm eq}, \tag{8}$$

where the subscripts "st" and "eq," respectively, refer to the limits $\tilde{t}_w\to 0$ and ∞ for χ_ω. The aging time dependence of τ is chosen as

$$\tau(\tilde{t}_w)=\{\tau_{\rm st}-\tau_{\rm fn}\}f(\tilde{t}_w)+\tau_{\rm fn}, \tag{9}$$

where $\tau_{\rm st}$ and $\tau_{\rm fn}$ are fit parameters *independent* of frequency ω. The normalized function $f(s)$ is chosen to have limiting values 1 and 0 for $s\to 0$ and ∞, respectively. In particular, we make the choice [15] $f(s)=a_o/[1+\exp\{s/\tau(s)\}^\beta]$, where $a_0=2^\beta$ is a normalization constant. Using this form of the $\tau(\tilde{t}_w)$ we have fitted $\chi_\omega(\tilde{t}_w)$ for all the different frequencies with a single (frequency-independent) stretching exponent β. In Fig. 3, a scaled plot of the different frequency data with respect to $\tilde{t}_w$ is displayed. The data sets for all the frequencies merge on a single master curve with $\beta=0.50$ shown as a solid line. The frequency range over which the data are fitted is restricted by two limiting conditions. ω should be below the microscopic peak in χ_ω representing the short-time dynamics. On the other hand on the low-frequency side ω is restricted by the maximum time to which we can extend the numerical solution scheme. In the present theoretical calculation, we are able to cover the range $t_w=2^m\Delta_0$ for $m=29$–42, for $\Delta_0=10^{-7}$, the above range equals to $t_w\approx 54$–439 805 covering the corresponding frequency range from 10^{-1} to 10^{-5} in the dimensionless units of the bare transport coefficient Γ_0. For the dielectric loss data, Lunkenheimer *et al.* in Ref. [10] use a somewhat different fitting scheme with the $f(s)$ in Eq. (9) being a stretched exponential function $\exp\{-[s/\tau(s)]^\beta\}$. Relaxation data when fitted with this scheme obtain the exponent (also frequency independent) $\beta=0.48$. In the inset of Fig. 3, the τ's from both of the above described fitting schemes are displayed. Both fitting schemes suggest qualitatively similar behavior in which aging accelerates with time. After the initial stage the waiting time dependence of the response function is close to the simple KWW with a constant relaxation time.

We now consider the FDT violation in the nonequilibrium state. The latter is generalized in terms of a quantity $X(t,t')$ (for $t>t'$) as $k_BTR(t,t')=X(t,t')\partial C(t,t')/\partial t'$. In the limit $t,t'\to\infty$, it is assumed that $X(t,t')\equiv x[C(t,t')]$ representing FDT violation in the correlation windows rather than time windows. For convenience of discussion, an integrated response function $F(t,t')$ is defined

$$F(t,t') \equiv -\int_{t'}^{t} dsR(t,s) = -\frac{1}{k_B T}\int_{C}^{1} x(\bar{C})d\bar{C}. \qquad (10)$$

If the FDT holds, $x=-1$ and the above relation reduces to $k_B TF(t)=C(t)-1$, using $C(t,t)=1$. An effective temperature $T_{\rm eff}$ for the nonequilibrium state is defined in terms of the ratio of the Fourier transforms, $k_B TF(\omega,t_w)/C(\omega,t_w)$. If the FDT holds, $T_{\rm eff}=1$. Using relation (7), we obtain that the choice $a_2=0.5$ and $a_3=3.0$ in the $p23$ model makes $T_{\rm eff}$ close to the experimental result of Ref. [16]. More importantly, the time scale of $\tilde{t}_w$ over which the cross over from the FDT to the aging regime occurs according to the present model is comparable with experimental observations as shown in Fig. 4. We also display in the inset of this figure the FDT violation corresponding to the case of Fig. 2 as seen from the correlation windows. This is similar to results [17] from molecular dynamics simulations of the binary Lennard-Jones mixtures.

The present model for an amorphous solid can be justified from a semimicroscopic basis. The potential energy is expressed as a Born–von Karman-type expansion of the coordinates $\{r_i\}$ of the N particles,

$$H = \sum_{ij}{}' J_{ij}^{(2)} u_i u_j + \sum_{ijk}{}' J_{ijk}^{(3)} u_i u_j u_k + \cdots + G(u_i), \qquad (11)$$

where $r_i=r_i^0+u_i$. The primes in the summations in the right-hand side indicate that the terms having all the corresponding running indices i,j,k, etc. being the same are absent. In the case of the amorphous solid, $\{r_i^0\}$ constitute a random structure corresponding to a local minimum of potential energy and u_i is the displacement of the ith particle from its parent site. The expansion in terms of u_i's is valid over the time scale of the structural relaxation. The single-site potential $G(u_i)$ [9] in the right-hand side of Eq. (11) is being included to stabilize the system. We will approximate $U=\Sigma_{i<j}\phi_{ij}$ as a sum of two-body potentials and write the potential energy in the translationally invariant form given by Eq. (1) by assuming $J_{ijk}^{(3)}=J_{ij}^{(3)}\delta_{jk}+J_{jk}^{(3)}\delta_{ki}+J_{ki}^{(3)}\delta_{ij}$, $J_{ji}^{(p)}=(-1)^p J_{ij}^{(p)}$, etc. For reaching expression (1) the coefficients of the single-site term $G(u_i)=\Sigma_i\{w_{2i}u_i^2+w_{3i}u_i^3+\cdots\}$ are chosen as $w_{2i}=-\Sigma_j' J_{ij}^{(2)}$, $w_{3i}=-\Sigma_{j,k}' J_{ijk}^{(3)}$, etc. The semimicroscopic interpretation described above is useful in linking the model with thermodynamic parameters [18]. This will test further the possibility of using the mode-coupling approach to study the complex dynamics of the nonequilibrium state of an amorphous solid.

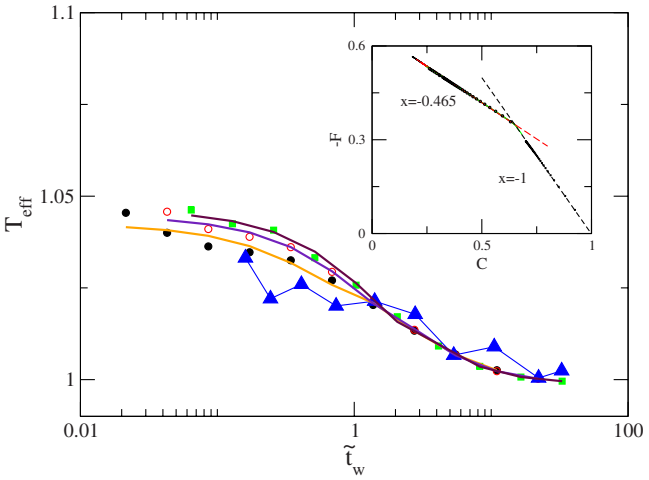

FIG. 4. (Color online) Effective temperature $T_{\rm eff}$ (see text) vs waiting times $\tilde{t}_w$ for $\omega=10^{-5}$ (filled circle), 3×10^{-4} (open circle), and 5×10^{-4} (filled square) in units of. Solid line corresponds to best-fit curve of theoretical results. Experimental data of Ref. [16] shown with filled triangles. Inset shows $-F(t+t_w,t_w)$ vs $C(t+t_w),t_w$ corresponding to the data of Fig. 2. The slope in the FDT violation regime is $x=-0.465$.

CSIR India is acknowledged for financial support.

[1] M. D. Ediger, C. A. Angell, and S. R. Nagel, J. Phys. Chem. **100**, 13200 (1996).
[2] L. C. E. Struik, *Physical Aging in Amorphous Polymers and Other Materials* (Elsevier, New York, 1978).
[3] T. R. Kirkpatrick and D. Thirumalai, Phys. Rev. B **36**, 5388 (1987).
[4] S. P. Das, Rev. Mod. Phys. **76**, 785 (2004).
[5] L. F. Cugliandolo and J. Kurchan, Phys. Rev. Lett. **71**, 173 (1993); J. Phys. A **27**, 5749 (1994).
[6] J. P. Bouchaud, J. Phys. I **2**, 1705 (1992).
[7] A. Crisanti and H.-J. Sommers, Z. Phys. B: Condens. Matter **87**, 341 (1992).
[8] L. F. Cugliandolo, in *Slow Relaxations and Nonequilibrium Dynamics in Condensed Matter, Session LXXVII, Les Houches 2002*, edited by J.-L. Barrat, M. V. Feigelman, J. Kurchan, and J. Dalibard (Springer, Berlin, 2003).
[9] R. Kühn and U. Horstmann, Phys. Rev. Lett. **78**, 4067 (1997); R. Kühn, Europhys. Lett. **62**, 313 (2003).
[10] P. Lunkenheimer, R. Wehn, U. Schneider, and A. Loidl, Phys. Rev. Lett. **95**, 055702 (2005).
[11] P. C. Martin, E. D. Siggia, and H. A. Rose, Phys. Rev. A **8**, 423 (1973); R. V. Jensen, J. Stat. Phys. **25**, 183 (1981).
[12] W. Gőtze and L. Sjőgren, Rep. Prog. Phys. **55**, 241 (1992); B. Kim and G. F. Mazenko, Phys. Rev. A **45**, 2393 (1992).
[13] L. Berthier, G. Biroli, J.-P. Bouchaud, W. Kob, K. Miyazaki, and D. R. Reichman, J. Chem. Phys. **126**, 184504 (2007).
[14] B. Kim and A. Latz, Europhys. Lett. **53**, 660 (2001); A. Andreanov and A. Lefèvre, *ibid.* **76**, 919 (2006).
[15] B. Sen Gupta and S. P. Das, Phys. Rev. E **76**, 061502 (2007).
[16] T. S. Grigera and N. E. Israeloff, Phys. Rev. Lett. **83**, 5038 (1999).
[17] W. Kob and J.-L. Barrat, Phys. Rev. Lett. **78**, 4581 (1997).
[18] S. P. Singh and S. P. Das (unpublished).